INT. J. HYPERTHERMIA, 1995, VOL. 11, NO. 2, 267–285

Application of the time-dependent Green's function and Fourier transforms to the solution of the bioheat equation†

B. GAO, S. LANGER and P. M. CORRY*

Department of Radiation Oncology, 103-RST, William Beaumont Hospital, 3601 West Thirteen Mile Road, Royal Oak, Michigan 48073, USA

(*Received 16 September 1993; revised 20 April 1994; accepted 16 June 1994*)

A theory for solving the bioheat equation is developed using a time-dependent Green's function and Fourier transform techniques. The description of both steady-state and time-dependent data are placed into a single framework which can also describe the effects of inhomogeneous blood perfusion. The theory is illustrated by examples including the modelling of a thermal conduction hyperthermia system and a new RF interstitial sytem. A possibility for measuring the blood perfusion parameter and thermal conductivity from the steady state temperature distribution of a point source is also proposed.

Key words: Hyperthermia, bioheat equation, Green's function, Fourier transform, interstitial hyperthermia

1. Introduction

The bioheat equation (Pennes 1948) is the basis for our understanding of the kinetics of the tumour and tissue heating in hyperthermia treatments. The solution of this equation is important both for treatment planning and for the design of new clinical heating systems. Traditionally we have relied almost exclusively on finite-difference or finite-element methods for such solutions. This may be necessary when tissue parameters such as the thermal conductivity have large variations or discontinuities in the region of interest. However, for localized heating methods such as interstitial hyperthermia, spacial variations of the tissue parameters are usually small in the heated region, which provides an opportunity for a more analytic approach. The alternative we present here is a method based on the time-dependent Green's function and Fourier transform techniques. It is appealing theoretically because all desired information about the temperature distribution: its steady state and its time dependence after power-on or power-off, are contained in a single formula [(8) or (9)]. It is also the ideal method for deriving analytic results and for developing qualitative understandings.

The application of the time-dependent Green's function to the modelling of the bioheat equation is not new. An example can be found in the analysis of thermal washout data by Newman *et al.* (1990). However, without using the Fourier transforms, the Green's function formalism is difficult to implement numerically, and therefore not very useful for many practical situations. Our theoretical development is much more complete, including the formulation of a perturbation theory which deals with the spacial and temporal dependencies of blood perfusion.

2. General theory

Assuming a constant thermal conductivity, the bioheat equation is given by (Pennes 1948):

$$\rho c_p \frac{\partial T'}{\partial t} = k\nabla^2 T' - \mu_t(\mathbf{x}, t)(T' - T_b) + Q(\mathbf{x}, t). \tag{1}$$

*To whom correspondence should be addressed.

†This work was supported by grant CA44550 from the US National Cancer Institute.

Here T' is the tissue temperature, ρ and c_p are the density and the specific heat at constant pressure respectively, both of which will be taken as constants (since we have already assumed the thermal conductivity k to be a constant anyway). T_b is the blood temperature which is again taken to be a constant. $\mu_t(x, t) > 0$ is the blood perfusion parameter which can depend on both space and time. $Q(\mathbf{x}, t)$ is the power density that we are depositing in the medium. From (1), it is obvious that the blood perfusion term $-\mu_t(\mathbf{x}, t)(T' - T_b)$ plays the role of a heat sink for $T' > T_b$ and the role of a heat source for $T' < T_b$. Defining $T \equiv T' - T_b$, equation (1) can be rewritten as

$$\rho c_p \frac{\partial T}{\partial t} - k\nabla^2 T + \mu_t(\mathbf{x}, t)T = Q(\mathbf{x}, t). \tag{2}$$

Remember that (2) is a consequence of (1) upon choosing the blood temperature as the reference temperature, which may not always be the best choice, as is demonstrated in § 8. When a different reference point is chosen, the resulting equation is different from (2) (§ 8).

Under the assumption of an infinite medium, the boundary condition for (2) is

$$T(\mathbf{x}, t) \overset{|\mathbf{x}| \to \infty}{\to} 0, \tag{3}$$

i.e. the temperature approaches the blood temperature far away from the volume of power deposition (other types of boundary conditions will be discussed in § 8). We will also assume, for now, $\mu_t(\mathbf{x}, t) = \mu_0$ to be a constant and leave the discussion of space- and time-dependent blood perfusion to § 9. With these assumptions the solution of (2) is given by

$$T(\mathbf{x}, t) = \int d^3x' G(\mathbf{x}, t; x', 0)T_0(\mathbf{x}') + (1/\rho c_p)\int_0^\infty dt' \int d^3x' G(x, t; \mathbf{x}', t')Q(\mathbf{x}', t'), \tag{4}$$

where $T_0(\mathbf{x}')$ is the initial temperature distribution and $G(\mathbf{x}, t; \mathbf{x}', t')$ is the time-dependent Green's function defined as the solution of

$$\left[\frac{\partial}{\partial t} - \alpha\nabla^2 + (\mu_0/\rho c_p)\right] G(\mathbf{x}, t; \mathbf{x}', t') = \delta(\mathbf{x} - \mathbf{x}')\delta(t - t') \tag{5}$$

with the boundary condition

$$G(\mathbf{x}, t; \mathbf{x}', t') \overset{|\mathbf{x} - \mathbf{x}'| \to \infty}{\to} 0, \tag{6}$$

and $\alpha \equiv k/\rho c_p$. This Green's function is not difficult to find and is given by

$$G(\mathbf{x}, t; \mathbf{x}', t') = H(t - t')[4\pi\alpha(t - t')]^{-3/2} \exp\left[-\frac{(\mathbf{x} - \mathbf{x}')^2}{4\alpha(t - t')} - \frac{\mu_0}{\rho c_p}(t - t')\right], \tag{7}$$

where $H(t - t')$ is the Heaviside step function defined by $H(t - t') = 0$ for $t - t' < 0$; and $H(t - t') = 1$ for $t - t' > 0$. Substituting (7) into (4), we obtain

$$\begin{aligned} T(\mathbf{x}, t) = {} & \frac{1}{(4\pi\alpha t)^{3/2}} e^{-(\mu_0/\rho c_p)t} \int d^3x' T_0(\mathbf{x}') \exp\left[-\frac{(\mathbf{x} - \mathbf{x}')^2}{4\alpha t}\right] \\ & + \frac{1}{\rho c_p (4\pi\alpha)^{3/2}} \int_0^t dt' \frac{1}{(t - t')^{3/2}} e^{-(\mu_0/\rho c_p)(t - t')} \\ & \int d^3x' Q(\mathbf{x}', t') \exp\left[-\frac{(\mathbf{x} - \mathbf{x}')^2}{4\alpha(t - t')}\right]. \end{aligned} \tag{8}$$

Given the initial temperature distribution and power deposition, this equation yields the temperature distribution at any time $t > 0$. In this sense it is the only equation needed for an infinite homogenous medium. From the computational point of view, however, (8) may be difficult to use, especially if the power deposition Q is not analytically known. To this end we take the Fourier transform of (8) and arrive at (Appendix)

$$\tilde{T}(\mathbf{s}, t) = \exp\left[-\left(\frac{\mu_0}{\rho c_p} + s^2\alpha\right)t \right]\tilde{T}_0(\mathbf{s}) + \frac{1}{\rho c_p}\int_0^t dt' \exp\left[-\left(\frac{\mu_0}{\rho c_p} + s^2\alpha\right)(t - t') \right]\tilde{Q}(\mathbf{s}, t'), \tag{9}$$

where tilde means the spacial Fourier transform which is defined for an arbitrary function F by

$$\tilde{F}(\mathbf{s}, t) \equiv \int d^3x e^{i\mathbf{s}\cdot\mathbf{x}} F(\mathbf{x}, t). \tag{10}$$

Equation (9) translate the convolution integrals in (8) into much simpler operations in the Fourier space (Appendix).

Once we have $\tilde{T}(\mathbf{s}, t)$, the temperature distribution $T(\mathbf{x}, t)$ is given by its inverse Fourier transform:

$$T(\mathbf{x}, t) = (2\pi)^{-3}\int d^3s e^{-i\mathbf{s}\cdot\mathbf{x}}\tilde{T}(\mathbf{s}, t). \tag{11}$$

The integration over time that remains in (9) can be easily carried out for most cases of interest. For example, if the power deposition $Q(\mathbf{x}, t)$ is turned on suddenly and remains a constant afterwards, we obtain

$$\tilde{T}(\mathbf{s}, t) = \exp\left[-\left(\frac{\mu_0}{\rho c_p} + s^2\alpha\right)t \right]\tilde{T}_0(\mathbf{s}) + \frac{1}{k}\frac{1}{s^2 + \mu_0/k}\left\{1 - \exp\left[-\left(\frac{\mu_0}{\rho c_p} + s^2\alpha\right)t \right]\right\}\tilde{Q}(\mathbf{s}), \tag{12}$$

which can be implemented using the Fast Fourier Transform (FFT) algorithm (Press *et al.* 1992). Specifically, we use the FFT to calculate $\tilde{T}_0(\mathbf{s})$ and $\tilde{Q}(\mathbf{s})$ from the initial temperature distribution $T_0(\mathbf{x})$ and the power deposition $Q(\mathbf{x})$ respectively. Substitution into equation (12) gives us $\tilde{T}(\mathbf{s}, t)$ at any desired time $t > 0$. The temperature distribution at time t: $T(\mathbf{x}, t)$, is then given by the inverse FFT of $\tilde{T}(\mathbf{s}, t)$.

Upon examining (12), we see that one of the important parameters characterizing the bioheat equation is $\rho c_p/\mu_0$, which gives the time scale on which steady-state is reached. With the parameters given in Table 1, it amounts to about 10 min. Another important parameter, which will become clearer in the next section, is $(k/\mu_0)^{1/2}$ which gives a length scale characterizing the range of influence. It is important to keep them in mind for a good qualitative understanding of the bioheat equation.

Table 1. Parameters.

k	$6{\cdot}0 \times 10^{-3}$ W cm^{-1} K^{-1}
μ_0	$6{\cdot}7 \times 10^{-3}$ W cm^{-3} K^{-1}
ρ	1·0 g cm^{-3}
c_p	4·0 J g^{-1} K^{-1}
σ	0·01 mho cm^{-1}

The following sections will be the application and generalization of what has been developed here. The parameters k, c_p, ρ, and μ_0 that we will use are those given in Table 1 unless stated otherwise.

3. Steady state

The steady-state temperature distribution is obtained by letting $t \to \infty$ in either (12) or (8). We obtain in Fourier space:

$$\tilde{T}^{st}(\mathbf{s}) = \frac{1}{k} \frac{1}{s^2 + \mu_0/k} \tilde{Q}(\mathbf{s}), \tag{13}$$

and in coordinate space:

$$T^{st}(\mathbf{x}) = \int d^3x' \frac{1}{4\pi k|\mathbf{x} - \mathbf{x}'|} \exp[-(\mu_0/k)^{1/2}|\mathbf{x} - \mathbf{x}'|] Q(\mathbf{x}'). \tag{14}$$

If the power deposition Q is independent of z, (14) reduces to

$$T^{st}(x, y) = \int dx' dy' \frac{1}{2\pi k} K_0\left((\mu_0/k)^{1/2}[(x - x')^2 + (y - y')^2]^{1/2}\right) Q(x', y'), \tag{15}$$

where $K_0(x)$ is the modified Bessel function of order zero (Abramowitz and Stegun 1964). If Q depends only on a single variable z, (14) reduces further to

$$T^{st}(z) = \int_{-\infty}^{\infty} dz' \frac{1}{2\sqrt{\mu_0 k}} \exp(-(\mu_0/k)^{1/2}|z - z'|) Q(z'). \tag{16}$$

Equations (14)–(16) are useful when the analytic expression for the power deposition is known. Otherwise direct application of (13) with a FFT algorithm is often more convenient. Here it should be pointed out that, as far as the steady-state temperature is concerned, the only relevant parameters are k and μ_0. The concept of SAR $(Q/\rho c_p)$ is not a very useful one here because it gives a false impression that the temperature depends on ρ and c_p. The importance of the parameter $(k/\mu_0)^{1/2}$ is quite clear from (14)–(16). It tells us that given power deposition at a certain point, how far its influence is going to reach. Furthermore, if two media have the same $(k/\mu_0)^{1/2}$, the steady-state temperature distribution induced in them by the same power deposition would differ by at most a multiplication constant.

In § 2 we made the assumption of an infinite medium. This actually means that the region of interest, i.e. the region where power is deposited, is away from any surfaces by a distance far greater than $(k/\mu_0)^{1/2}$ which amounts to 0·95 cm with the parameters given in Table 1.

4. A point source

The solution for a point source is of fundamental importance for all linear differential equations because of the superposition principle. Given such a solution, we can superimpose them to obtain the solution for a arbitrary source distribution. This is in fact the meaning of (14)–(16). For the bioheat equation, the solution for a point source $Q(\mathbf{x}) = P\delta(\mathbf{x} - \mathbf{x}_0)$ in an infinite homogeneous medium is given by

$$T^{st}(\mathbf{x}) = \frac{P}{4\pi k|\mathbf{x} - \mathbf{x}_0|} e^{-(\mu_0/k)^{1/2}|\mathbf{x} - \mathbf{x}_0|}, \tag{17}$$

where P is the total power of the point source. Note that (17) is basically a screened Coulomb potential, with screening provided by blood perfusion. This is one of the simplest solutions of the bioheat equation, and it suggests a simple way of measuring both the heat conductivity k and the perfusion parameter μ_0. By measuring the temperature at two different radii r_1 and r_2 from the source, we have from (17):

$$k = \frac{P}{4\pi r_1 T^{st}(r_1)} \exp\left\{\frac{r_1}{r_2 - r_1}[\ln(r_2/r_1) + \ln(T^{st}(r_2)/T^{st}(r_1))]\right\}, \tag{18}$$

and

$$\mu_0 = \frac{k}{(r_2 - r_1)^2}\{\ln(r_1/r_2) + \ln[T^{st}(r_1)/T^{st}(r_2)]\}^2. \tag{19}$$

The blood perfusion and thermal conductivity measured this way can have a spatial resolution of better than $(k/\mu_0)^{1/2}$, which is 0·95 cm with the parameters that we are using (Table 1). Better resolution can be achieved for greater perfusion.

5. Thermal conduction interstitial system

Here we consider a system made up of N parallel infinitely-long hot needles, which is a good approximation to the system under consideration if the needle spacing is small compared to their length. This assumption of parallel infinitely-long needles changes a complicated 3-D problem into a 2-D problem, greatly reducing the demands on computer power (all calculations presented in this paper were done on an IBM PC 386). Needle positions are specified by a set of parameters (x_i, y_i) for $i = 1, \ldots, N$. The radius of the needle is defined as r_n, assumed to be the same for all needles. While this latter assumption is not necessary, it is a practical reality. Our goal is to find the resulting steady-state temperature distribution $T^{st}(\mathbf{x})$ when the needles are kept at the constant temperature $T_i (i = 1, \ldots, N)$.

This desired temperature distribution can be found by solving a boundary value problem with the requirement that the temperature should be equal to the T_i on the surface of the i-th needle (Deford *et al.* 1990). There is however a much more efficient method for solving this problem. It is based on the idea of the effective source, very similar to the method of image charges in electrostatics (Jackson 1975).

Consider what happens if we replace the set of hot needles by a set of line (power) sources at the same positions:

$$Q(x, y) = \sum_{i=1}^{N} P_i \delta(x - x_i)\delta(y - y_i), \tag{20}$$

where P_i is the power deposition per unit length of the i-th line source which is left to be unknown at this point. Substituting (20) into (15), we obtain the steady-state temperature distribution T_P^{st} for the power deposition as given by (20):

$$T_P^{st}(x, y) = \frac{1}{2\pi k}\sum_{i}^{N} P_i K_0\left((\mu_0/k)^{1/2}[(x - x_i)^2 + (y - y_i)^2]^{1/2}\right), \tag{21}$$

where $K_0(x)$ is again the zeroth order modified Bessel function which can be evaluated rather easily (Abramowitz and Stegun 1964). The question is how the solution given by equation (21) is related to the desired solution $T^{st}(\mathbf{x})$ for hot needles. Since both $T_P^{st}(\mathbf{x})$ and $T^{st}(\mathbf{x})$ satisfy the same equation:

$$k\nabla^2 T - \mu_0 T = 0$$

outside the needles, they would be equal if a set of P_i can be found such that the boundary conditions on the hot needles can be satisfied. In cases where the radius of the needles is much smaller than their spacing, the boundary condition of fixed temperature $T_i (i = 1, \ldots, N)$ on the needles translates via (21) into the following set of linear equations for P_i:

$$\sum_{j=1}^{n} A_{ij} P_j = T_i, \tag{22}$$

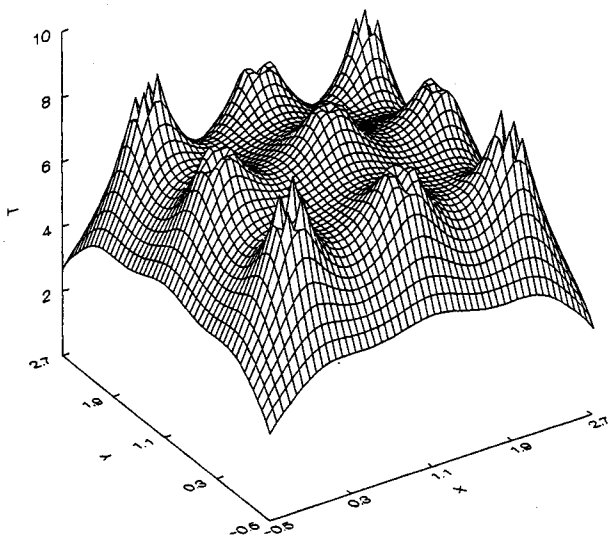

Figure 1. Steady-state temperature distribution for thermal conductive heating. All nine needles are maintained at 10°C above the blood temperature. X- and Y-axes units are cm. Temperature is in degrees above blood temperature. These axis dimensions also apply to Figures 2, 4, 5, 6 and 7.

with

$$A_{ij} = \frac{1}{2\pi k} K_0((\mu_0/k)^{1/2} d_{ij}), \tag{23}$$

where

$$d_{ij} = \begin{cases} [(x - x_i)^2 + (y - y_i)^2]^{1/2} & \text{for } i \neq j \\ r_n & \text{for } i = j \end{cases}. \tag{24}$$

The required temperature distribution $T^{st}(\mathbf{x})$ for hot needles is then given by (21) with P_i being the solution of (22). The essence of this approach is similar to that behind the method of image charges in electrostatic problems (Jackson 1975), i.e. to replace the boundary conditions by some effective sources outside the boundary (which in our case means inside the needles). This same idea will also be used in the next section for finding the power deposition and in § 8 for finding the Green's function for different boundary conditions.

Figure 1 shows the temperature distribution for a 9-needle configuration. The needles are distributed on a 3×3 rectangular grid with needle space of 1·1 cm and are maintained at 10°C above the blood temperature. The radius of the needles r_n is assumed to be 0·75 mm. These parameters are so chosen to compare the result of thermal conductive heating obtained here with that of RF heating to be discussed in the next section.

6. Interstitial RF system

In interstitial RF systems, heating is achieved by applying RF voltage on a set of implanted needles (Corry *et al.* 1993, Martinez *et al.* 1993). The power deposition is given by

$$Q(\mathbf{x}) = (\sigma/2)\mathbf{E}^*(\mathbf{x}) \cdot \mathbf{E}(\mathbf{x}), \tag{25}$$

where $\mathbf{E}(\mathbf{x})$ is amplitude of the electric field (complex in general) at point $\mathbf{x}$ as a result of applied voltage; σ is the electric conductivity (which may be frequency-dependent at higher RF frequencies). Due to the large RF wavelength, the determination of the electric field can be treated as an electrostatic problem. Assuming the needles to be infinitely long and the

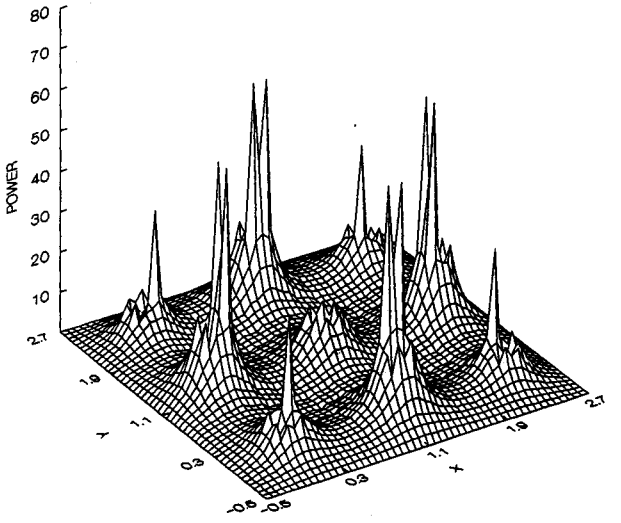

Figure 2. Power deposition resulting from interstitial RF heating in a nine needle configuration. The voltage pattern is shown in Figure 3. Power density is given in units of W/cm^3.

dielectric constant to be position-independent in the volume of interest, the electric field amplitude is given by

$$\mathbf{E}(\mathbf{x}) = \sum_{i=1}^{N} \bar{q}_i \frac{(x-x_i)\hat{x} + (y-y_i)\hat{y}}{(x-x_i)^2 + (y-y_i)^2}, \tag{26}$$

where $\bar{q}_i = q_i/2\pi\varepsilon$ is what we will call the reduced charge on needle i, with q_i being the amplitude of actual charge on needle i. $\hat{x}$ and $\hat{y}$ are the unit vectors in the x- and y-direction respectively. In obtaining (26) we have made use of the fact that the radius of the needle (0·75 mm) is much smaller than needle spacing (1·1 cm). Reduced charges on needles can be found using voltage differences as input and the fact that the sum of charges on all needles is zero. We obtain

$$\sum_{j=1}^{N} A_{ij}\bar{q}_j = b_i. \tag{27}$$

Taking an arbitrary needle with index i_R to be the reference needle (to which all voltage differences are referred), the elements of A and b are given by

$$A_{ij} = \begin{cases} \ln(d_{iR_j}/d_{ij}) & \text{for } i \neq i_R \\ 1 & \text{for } i = i_R \end{cases}. \tag{28}$$

and

$$b_i = V_i - V_{i_R}. \tag{29}$$

Here V_i is the voltage of the i-th needle. V_{i_R} is the voltage on the reference needle. d_{ij} is defined in the same way as in (24). Note that the power deposition is independent of the dielectric constant (under our assumption that it is a constant in the volume of interest).

Figure 2 shows the power deposition pattern calculated for a 9-needle configuration. The needles are distributed on a 3×3 grid with a spacing of 1·1 cm, and the voltage pattern is shown in Figure 3 with $V_{+-} = 50$ Volts. Figure 4 shows the corresponding steady-state temperature distribution. It is calculated by using FFT and (13). It is smoother than what was achieved by thermal conductive heating (Figure 1) because the power deposition as

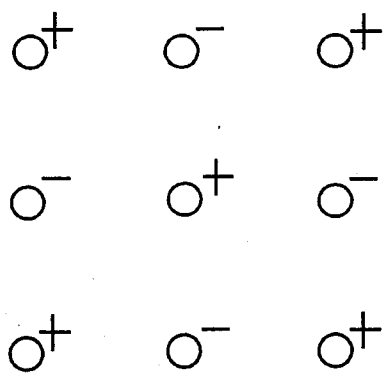

Figure 3. One of the possible voltage patterns for a nine needles interstitial RF heating configuration.

shown in Figure 2 is more diffuse than the equivalent power deposition for thermal conductive heating. Figures 5–7 show the temperature distribution at 1, 4, and 12 min after power is turned on. They are obtained from (12) using FFT. Note how the temperature distribution is gradually smoothed out by thermal conduction.

7. Description of 'thermal washout'

The term 'thermal washout' refers to the decay of temperature after the power deposition is turned off. For an infinite homogeneous medium, this process is described by the first term of (8) or (9). That is

$$T(\mathbf{x}, t) = \frac{1}{(4\pi\alpha t)^{3/2}} e^{-(\mu_0/\rho c_p)t} \int d^3x' T_0(\mathbf{x}') \exp\left[-\frac{(\mathbf{x}-\mathbf{x}')^2}{4\alpha t}\right], \tag{30}$$

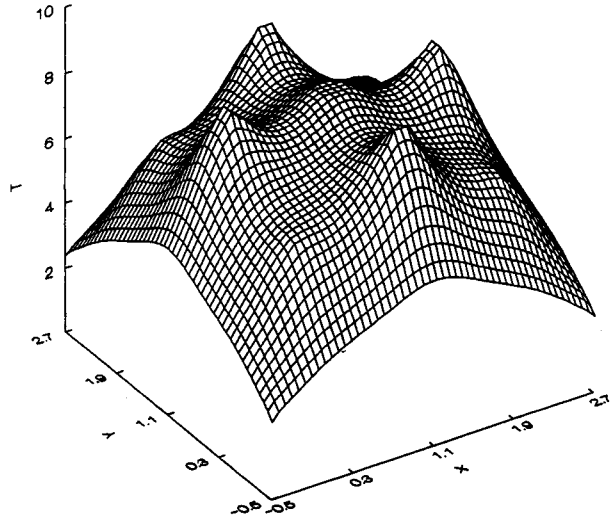

Figure 4. The steady-state temperature distribution resulting from the power deposition as shown in Figure 2. All temperature distributions are given in units of degrees C above the blood temperature.

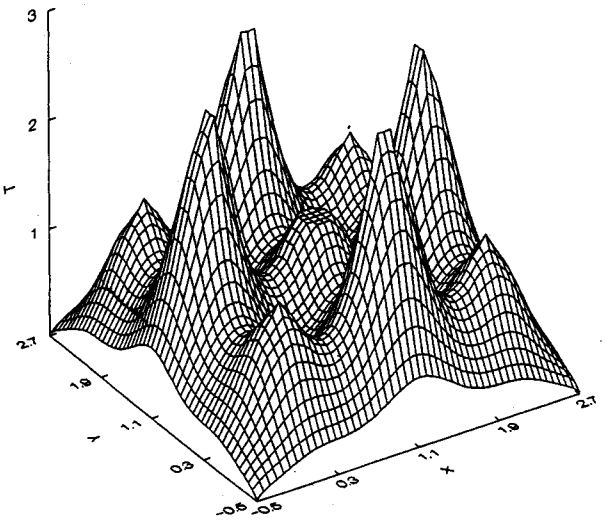

Figure 5. Temperature distribution 1 min after the power deposition as shown in Figure 2 is turned on.

or in terms of Fourier transforms

$$\tilde{T}(s, t) = \exp\left[-\left(\frac{\mu_0}{\rho c_p} + s^2\alpha\right)t \right]\tilde{T}_0(\mathbf{s}). \tag{31}$$

The important point here is that the time dependence of the temperature at point **x** depends not only on the tissue parameters (including perfusion), but also on the whole initial temperature distribution. The time dependence is *not* a simple exponential function unless the initial temperature distribution is uniform. Take, for example, a Gaussian distribution:

$$T_0(\mathbf{x}) = T_0 \exp\left[-(\mathbf{x} - \mathbf{x}_0)^2/\sigma \right]. \tag{32}$$

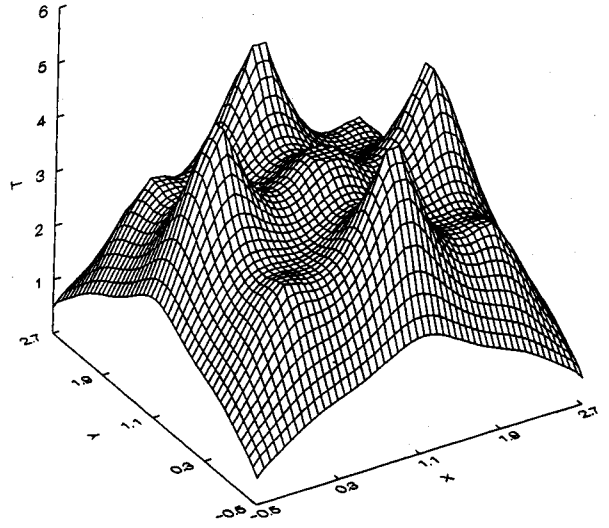

Figure 6. Temperature distribution 4 min after the power deposition as shown in Figure 2 is turned on.

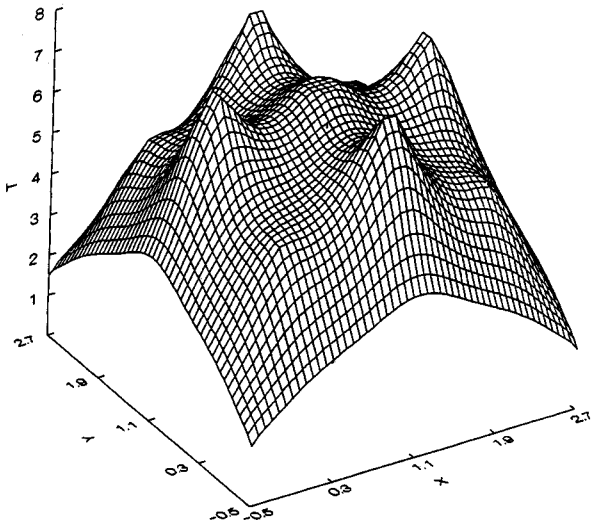

Figure 7. Temperature distribution 12 min after the power deposition as shown in Figure 2 is turned on.

From (30) we obtain

$$T(\mathbf{x}, t) = T_0 e^{-(\mu_0/\rho c_p)t}\left(\frac{\sigma}{\sigma + 4\alpha t}\right)^{3/2} \exp[-(\mathbf{x} - \mathbf{x}_0)^2/(\sigma + 4\alpha t)]. \tag{33}$$

The time dependence is obviously not a simple exponential unless the limit of $\sigma \to \infty$ (the uniform temperature limit) is taken. Another example is where the initial temperature distribution is the steady-state solution for a point source, (17). The corresponding temperature distribution after power-off is given in this latter case by

$$T(\mathbf{x}, t) = \frac{P}{4\pi k|\mathbf{x} - \mathbf{x}_0|}\frac{1}{2}\{e^{-(\mu_0/k)^{1/2}|\mathbf{x} - \mathbf{x}_0|}[1 - \Phi((\mu_0 t/\rho c_p)^{1/2} - |\mathbf{x} - \mathbf{x}'|/(4\alpha t)^{1/2})]$$
$$- e^{(\mu_0/k)^{1/2}|\mathbf{x} - \mathbf{x}_0|}[1 - \Phi((\mu_0 t/\rho c_p)^{1/2} + |\mathbf{x} - \mathbf{x}'|/(4\alpha t)^{1/2})]\}, \tag{34}$$

where $\Phi(x) \equiv 2/\sqrt{\pi}\int_0^x e^{-t^2}dt$ is the error function (Abramowitz and Stegun 1964). Again the time dependence is far from a simple exponential. It therefore appears that thermal washout is in general not a good method for obtaining accurate tissue parameters (Newman *et al.* 1990). The 'modified thermal clearance' technique proposed by Waterman *et al.* (1991), while avoiding these theoretical problems, is difficult to implement clinically and very susceptible to any error in the positioning of temperature probes.

8. Effects of boundary conditions

Up to this point our approach has been based on the assumption of an infinite homogeneous medium. Modifications are required when this condition is violated. An interesting case to consider here is heating near the surface of the skin, which will be treated as a plane at $z = 0$ with the z-axis being perpendicular to the surface and pointing into the body. Given some initial temperature distribution $T_0'(\mathbf{x})$ and power deposition $Q'(\mathbf{x}, t)$ inside the body, i.e. in the region $z > 0$, we seek the temperature distribution $T(\mathbf{x}, t)$ inside the body at subsequent times.

Following Newman *et al.* (1990), we consider both adiabatic and isothermal boundary conditions. The adiobatic boundary condition is closer to reality and is specified by

$$\frac{\partial}{\partial z}T(\mathbf{x}, t)\bigg|_{z=0} = 0. \tag{35}$$

This boundary condition is a good approximation to the actual clinical situation if the medium in contact with the body (e.g. air) has very small thermal conductivity. It is easy to show that the time-dependent Green's function is given in this case by

$$G'(\mathbf{x}, t; \mathbf{x}', t') = H(t-t')[4\pi\alpha(t-t')]^{3/2}\exp\left[-\frac{\mu_0}{\rho c_p}(t-t')\right] \times\left\{\exp\left[-\frac{(x-x')^2+(y-y')^2+(z-z')^2}{4\alpha(t-t')}\right] + \exp\left[-\frac{(x-x')^2+(y-y')^2+(z+z')^2}{4\alpha(t-t')}\right]\right\} \tag{36}$$

Equation (4) still applies except that G, T_0 and Q are replaced by G', T_0', and Q' respectively, and that the volume integral over the whole space is replaced by the volume integral over the region with $z \geq 0$ only. The temperature distribution obtained upon substituting (36) into (4) can be written in exactly the same form as (8) if we define Q and T_0 as

$$Q(\mathbf{x}) = \begin{cases} Q'(x, y, z) & \text{for } z \geq 0 \\ Q'(x, y, -z) & \text{for } z < 0 \end{cases}, \tag{37}$$

$$T_0(\mathbf{x}) = \begin{cases} T_0'(x, y, z) & \text{for } z \geq 0 \\ T_0'(x, y, -z) & \text{for } z < 0 \end{cases}, \tag{38}$$

The same is true for all other formulae, (9), (12)–(16), (30), and (31), derived in §§ 2, 3, and 7. This equivalence implies that if we replace the real power deposition Q' and the real initial temperature distrubition T_0' by the effective ones defined by (37) and (38), we can ignore the boundary condition, equation (35), and solve the problem as if we had an infinite homogeneous medium. Take for example the systems we discussed in §§ 5 and 6 in which the needles are assumed to be infinitely long. A better model may assume that needles are 'half' infinitely long, starting from the places where they enter the skin. Under the adiabatic boundary condition, such a model would however not change our earlier results in any way as long as the needles are inserted perpendicular to the surface, a conclusion which we can reach immediately from (37) and (38). As another example, let us consider the heating due to a plane propagating microwave. Upon normal incidence to the surface, the power deposition is given by

$$Q'(\mathbf{x}) = Q_0 e^{-\gamma z} \quad \text{for } z \geq 0, \tag{39}$$

where γ is a tissue- and frequency-dependent parameter. The effective power deposition is therefore [from equation (37)]:

$$Q(\mathbf{x}) = \begin{cases} Q_0 e^{-\gamma z} & \text{for } z \geq 0 \\ Q_0 e^{\gamma z} & \text{for } z < 0 \end{cases},$$

or simply

$$Q(\mathbf{x}) = Q_0 e^{-\gamma|z|}.$$

The steady-state temperature distribution for plane-wave microwave heating is obtained by substituting the effective power deposition into (16). We obtain:

$$T^{st}(z) = \frac{Q_0}{\mu_0 - k\gamma^2}(e^{-\gamma z} - \gamma(\mu_0/k)^{-1/2} e^{-(\mu_0/k)^{1/2} z}). \tag{40}$$

Here again the reference temperature (the zero point) has been taken to be the blood temperature. From this equation we see that under the adiabatic boundary condition, (35),

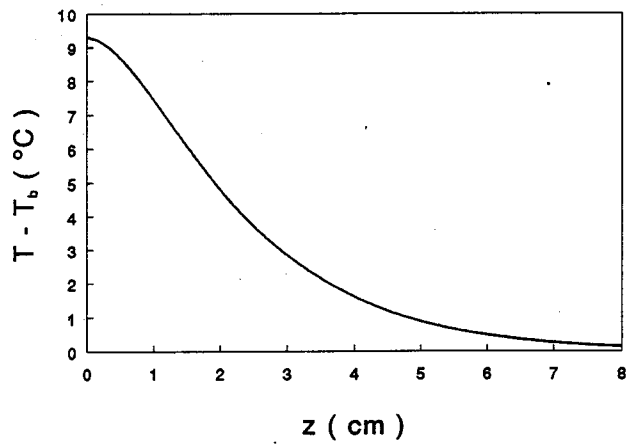

Figure 8. Temperature distribution as given by equation (40) for microwave (915 MHz) heating under the adiabatic boundary condition. $z = 0$ refers to the surface of skin.

the temperature is equal to the blood temperature everywhere inside the body in the absence of any heating ($Q_0 = 0$). Figure 8 shows the temperature distribution given by (40) for $Q_0 = 0{\cdot}1$ W/cm^3; $\gamma = 0{\cdot}64$ cm^{-1} [for microwaves at a frequency of 915 MHz (Newman *et al.* 1990)]; and other parameters as given in Table 1.

The second type of boundary condition, isothermal, is specified by

$$T'(\mathbf{x}, t)|_{z=0} = T_s. \tag{41}$$

This type of boundary condition is appropriate if the medium in contact with the body is a good heat conductor maintained at a constant temperature (such as an ice pad). In this case it is much more convenient to take T_s instead of T_b as the reference temperature, so that the boundary condition can be written as

$$T(\mathbf{x}, t)|_{z=0} = 0 \tag{42}$$

by defining $T \equiv T' - T_s$. Such a choice invalidates (2) which is derived from (1) upon taking the blood temperature as the reference temperature. With our new choice of T_s as the reference temperature, i.e. defining $T \equiv T' - T_s$, (1) becomes

$$\rho c_p \frac{\partial T}{\partial t} - k\nabla^2 T + \mu_0 T = Q'(\mathbf{x}, t) + \mu_0(T_b - T_s). \tag{43}$$

The last term in this equation is very important and cannot be ignored unless $T_b = T_s$. Without such a term, the temperature in the absence of power deposition ($Q \equiv 0$) would be equal to the surface temperature T_s everywhere inside the body, which is obviously incorrect because the temperature should of course approach the blood temperature T_b at depth. We point this out because it was ignored by Newman *et al.* (1990). The time-dependent Green's function for (43) with the boundary condition of (42) is given by

$$\begin{aligned} G'(\mathbf{x}, t; \mathbf{x}', t') = H(t-t')[4\pi\alpha(t-t')]^{3/2} \exp\left[-\frac{\mu_0}{\rho c_p}(t-t')\right] \\ \times \left\{ \exp\left[-\frac{(x-x')^2 + (y-y')^2 + (z-z')^2}{4\alpha(t-t')}\right] \right. \\ \left. - \exp\left[-\frac{(x-x')^2 + (y-y')^2 + (z+z')^2}{4\alpha(t-t')}\right] \right\} \end{aligned} \tag{44}$$

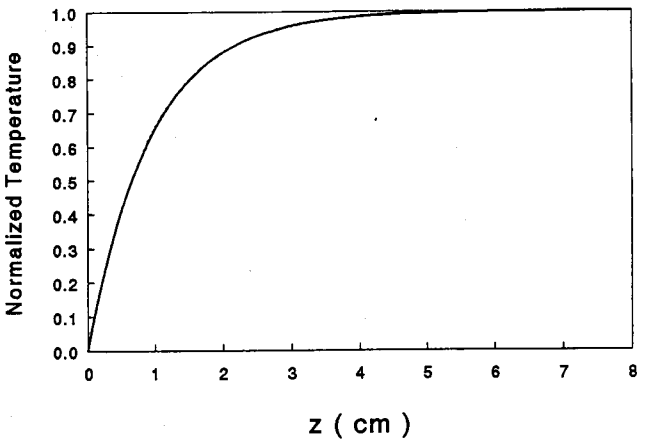

Figure 9. Normalized temperature distribution $T^{st}(z)/(T_b - T_s)$ in the absence of heating under the isothermal boundary condition. $z = 0$ refers to the surface of skin.

Equation (4) remains valid because of our choice of reference temperature. The formulae derived this way are again the same as those in §§ 2, 3, and 7 [(8)–(9), (12)–(16), and (32)–(33)] if we define the effective power deposition Q and effective initial temperature distribution T_0 as

$$Q(\mathbf{x}) = \begin{cases} Q'(x, y, z) + \mu_0(T_b - T_s) & \text{for } z \geq 0 \\ -Q'(x, y, -z) - \mu_0(T_b - T_s) & \text{for } z < 0 \end{cases}, \tag{45}$$

and

$$T_0(\mathbf{x}) = \begin{cases} T_0'(x, y, z) & \text{for } z \geq 0 \\ -T_0'(x, y, -z) & \text{for } z < 0 \end{cases}. \tag{46}$$

In the absence of any heating ($Q_0 = 0$), the effective power deposition is given by

$$Q(\mathbf{x}) = \begin{cases} +\mu_0(T_b - T_s) & \text{for } z \geq 0 \\ -\mu_0(T_b - T_s) & \text{for } z < 0 \end{cases}. \tag{47}$$

Since it is independent of x and y, the steady-state temperature distribution in the *absence* of heating is given by substituting (47) into (16). We arrive at:

$$T^{st}(z) = (T_b - T_s)(1 - e^{-(\mu_0/k)^{1/2}z}). \tag{48}$$

It approaches the blood temperature at depth as it should (remember that T_s has been taken as the reference temperature so $T_b - T_s$ is the blood temperature as referred to T_s). Figure 9 is a plot of the normalized temperature distribution $T^{st}(z)/(T_b - T_s)$. This solution actually tells us quite a bit, such as how much heat the body would lose to an ice pad or how much it would gain from a hot pad with temperature greater than T_b. They are determined by the heat flux at the boundary ($z = 0$) and are given by

$$-k\frac{\partial T}{\partial z}\bigg|_{z=0} = -(\mu k)^{1/2}(T_b - T_s) \tag{49}$$

$$= -6{\cdot}34 \times 10^{-3}(T_b - T_s)(\text{W/cm}^2), \tag{50}$$

where the parameters in Table 1 have been used. Taking $T_b = 37°\text{C}$ and $T_s = 0°\text{C}$, the heat flux amounts to $-0{\cdot}23$ W/cm^2. It means if we put an ice pad on our body, we would be losing heat at a rate of 0·23 Joule per s per square cm.

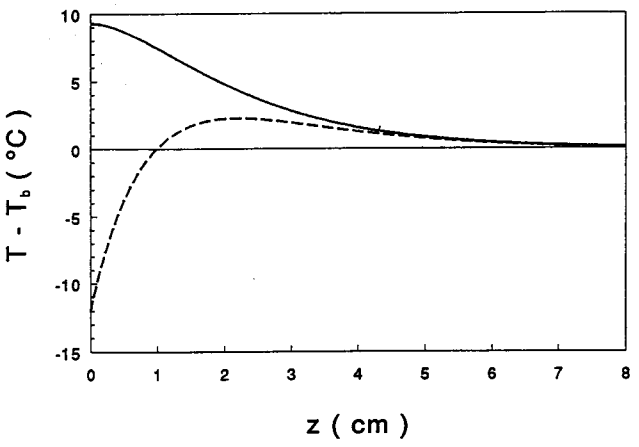

Figure 10. Temperature distribution as given by equation (52) for microwave (915 MHz) heating under the isothermal boundary condition $T(z=0)=25°C$.

Now let us take another look at the microwave heating. For isothermal boundary conditions the effective power deposition is given by [from (45)]

$$Q(\mathbf{x}) = \begin{cases} Q_0 e^{-\gamma z} + \mu_0(T_b - T_s) & \text{for } z \geq 0 \\ -Q_0 e^{-\gamma z} - \mu_0(T_b - T_s) & \text{for } z < 0 \end{cases},$$

Substituting it into (16), we obtain

$$T^{st}(z) = (T_b - T_s)(1 - e^{-(\mu_0/k)^{1/2}z}) + \frac{Q_0}{\mu_0 - k\gamma^2}(e^{-\gamma z} - e^{-(\mu_0/k)^{1/2}z}). \tag{51}$$

Remember that the reference point for this temperature distribution is T_s instead of T_b. To compare it with the result of (40) we have to shift them to a common origin. In taking the blood temperature as the origin, (51) becomes

$$T^{st}(z) = -(T_b - T_s)e^{-(\mu_0/k)^{1/2}z} + \frac{Q_0}{\mu_0 - k\gamma^2}(e^{-\gamma z} - e^{-(\mu_0/k)^{1/2}z}), \tag{52}$$

which can now be compared with (40) directly. Figure 10 shows this comparison for $T_b = 37°C$ and $T_s = 25°C$. Other parameters are the same as those used to generate Figure 8. We see that near the surface of the skin, temperature distributions are drastically different for different boundary conditions. This big difference is related intimately to the fact that for microwave heating, considerable power deposition is near the surface where the effects of boundary conditions are greatest. If all the power were deposited inside (compared to the characteristic distance $(k/\mu_0)^{1/2}$), different boundary conditions would not have made much difference.

9. Effects of inhomogeneous blood perfusion

In a real world situation, blood perfusion can be a function of both space and time. It can be written generally as

$$\mu(\mathbf{x}, t) \equiv \mu_0 + \Delta\mu(\mathbf{x}, t), \tag{53}$$

where μ_0 would represent some sort of average, and $\Delta\mu_t$ represents the deviation from this average. In the case of an infinite homogenous medium, equation (2) becomes

$$\rho c_p \frac{\partial T}{\partial t} - k\nabla^2 T + \mu_0 T = Q(\mathbf{x}, t) - \Delta\mu(\mathbf{x}, t)T. \tag{54}$$

With the help of the time-dependent Green's function, it can be rewritten as an integral equation:

$$T(\mathbf{x}, t) = \int d^3x' G(\mathbf{x}, t; \mathbf{x}', 0) T_0(\mathbf{x}') + (1/\rho c_p) \int_0^\infty dt' \int d^3x' G(\mathbf{x}, t; \mathbf{x}', t') Q(\mathbf{x}', t')$$

$$- (1/\rho c_p) \int dt' \int d^3x' G(\mathbf{x}, t; \mathbf{x}', t') \Delta\mu(\mathbf{x}', t') T(\mathbf{x}', t'), \tag{55}$$

which can then be solved by iteration. The zeroth order solution is given by

$$T^{(0)}(\mathbf{x}, t) = \int d^3x' G(\mathbf{x}, t; \mathbf{x}', 0) T_0(\mathbf{x}') + (1/\rho c_p) \int_0^\infty dt' \int d^3x' G(\mathbf{x}, t; \mathbf{x}', t') Q(\mathbf{x}', t'). \tag{56}$$

In other words, the space- and time-dependent part of the perfusion is ignored in this order. The solution to the first order in $\Delta\mu$ is obtained by substituting the zeroth order solution back into the left hand side (LHS) of (55). We obtain

$$T^{(1)}(\mathbf{x}, t) = T^{(0)}(\mathbf{x}, t) - (1/\rho c_p) \int_0^\infty dt' \int d^3x' G(\mathbf{x}, t; \mathbf{x}', t') \Delta\mu(\mathbf{x}', t') T^{(0)}(\mathbf{x}', t'). \tag{57}$$

The n-th order solution is obtained by substituting the (n − 1)-th order solution into LHS of (55). The result is

$$T^{(n)}(\mathbf{x}, t) = T^{(0)}(\mathbf{x}, t) - (1/\rho c_p) \int_0^\infty dt' \int d^3x' G(\mathbf{x}, t; \mathbf{x}', t') \Delta\mu(\mathbf{x}', t') T^{(n-1)}(\mathbf{x}', t'). \tag{58}$$

Equation (57) is of course only a special case of (58). In this way, starting from the zeroth order solution (in which variation of blood perfusion is ignored), we can successively improve our solution by going to higher order perturbations. It is obvious that the n-th order correction is of the order of $O(\Delta\mu^n)$. If the variation of blood perfusion is small, the first order solution would often be sufficient.

If $\Delta\mu$ is time-independent and we are interested in only the steady-state temperature distribution, (58) reduce to (we already know how to find the zeroth order solution from § 3):

$$T^{st(n)}(\mathbf{x}) = T^{st(0)}(\mathbf{x}) - \int d^3x' \frac{1}{4\pi k|\mathbf{x} - \mathbf{x}'|} \exp[-(\mu_0/k)^{1/2}|\mathbf{x} - \mathbf{x}'|] \Delta\mu(\mathbf{x}') T^{st(n-1)}(\mathbf{x}'). \tag{59}$$

Again the convolution integrals in these equations can be dealt with by Fourier transform if analytical integration is not possible.

The cases of other boundary conditions can be dealt with in a similar fashion. We obtain for the steady-state temperature distribution:

$$T^{st(0)}(\mathbf{x}) = \int d^3x' \frac{1}{4\pi k|\mathbf{x} - \mathbf{x}'|} \exp[-(\mu_0/k)^{1/2}|\mathbf{x} - \mathbf{x}'|] Q(\mathbf{x}'), \tag{60}$$

and

$$T^{st(n)}(\mathbf{x}) = T^{st(0)}(\mathbf{x}) - \int d^3x' \frac{1}{4\pi k|\mathbf{x} - \mathbf{x}'|} \exp[-(\mu_0/k)^{1/2}|\mathbf{x} - \mathbf{x}'|] S^{(n-1)}(\mathbf{x}'), \tag{61}$$

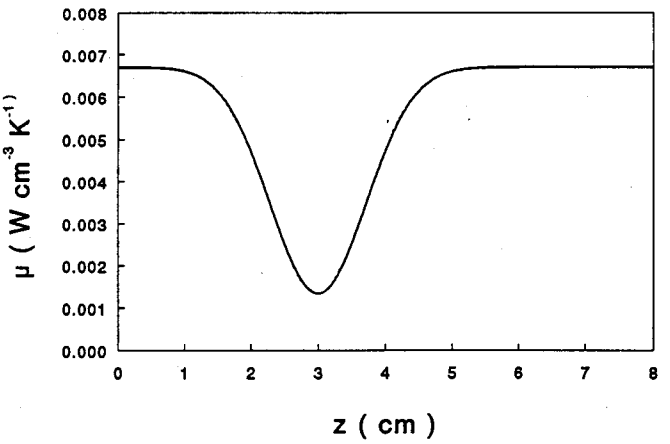

Figure 11. Assumed blood perfusion parameter.

where $Q(\mathbf{x})$ is given by (37) for the adiabatic boundary condition and by

$$Q(\mathbf{x}) = \begin{cases} Q'(x, y, z) + \mu(x, y, z)(T_b - T_s) & \text{for } z \geq 0 \\ -Q'(x, y, -z) - \mu(x, y, -z)(T_b - T_s) & \text{for } z < 0 \end{cases} \tag{62}$$

for the isothermal boundary condition. $S_I^{(n)}(\mathbf{x})$ is defined by

$$S_I^{(n)}(\mathbf{x}) = \begin{cases} \Delta\mu(x, y, z) T^{st(n)}(x, y, z) & \text{for } z \geq 0 \\ \Delta\mu(x, y, -z) T^{st(n)}(x, y, -z) & \text{for } z < 0 \end{cases} \tag{63}$$

for the adiabatic boundary condition, and by

$$S_I^{(n)}(\mathbf{x}) = \begin{cases} \Delta\mu(x, y, z) T^{st(n)}(x, y, z) & \text{for } z \geq 0 \\ -\Delta\mu(x, y, -z) T^{st(n)}(x, y, -z) & \text{for } z < 0 \end{cases} \tag{64}$$

for the isothermal boundary condition.

As a simple illustration, let us consider how the steady state temperature distribution as given by (40) (corresponding to microwave heating under the adiabatic boundary condition) would be affected by blood perfusion inhomogeneity which depends on z only. Specifically we will take

$$\Delta\mu(z) = -0{\cdot}8\mu_0 e^{-(z - z_0)^2/\sigma_1}, \tag{65}$$

with $z_0 = 3{\cdot}0$ cm and $\sigma_1 = 1{\cdot}0$ cm^2. The resulting blood perfusion parameter $\mu(z) = \mu_0 + \Delta\mu(z)$ is plotted in Figure 10. Since both $\Delta\mu$ and $T^{st(n)}$ depend only on z, (61) becomes

$$T^{st(n)}(z) = T^{st(0)}(z) - \frac{1}{2\sqrt{\mu_0 k}} \int_{-\infty}^{\infty} dz' \exp(-(\mu_0/k)^{1/2}|z - z'|) S_I^{st(n-1)}(z'), \tag{66}$$

with

$$S_I^{(n)}(z) = \begin{cases} \Delta\mu(z) T^{st(n)}(z) & \text{for } z \geq 0 \\ \Delta\mu(-z) T^{st(n)}(-z) & \text{for } z < 0 \end{cases} \tag{67}$$

Figure 12 is the plot of steady-state temperature distributions obtained for different orders of approximation. Q_0 has been taken as 0·1 W/cm^3, γ as 0·64 cm^{-1} so that the zeroth order temperature distribution is the same as that of Figure 8. Note that even when the variation of blood perfusion is as large as shown in Figure 11, our perturbative expansion converges very quickly. The second order result is already very close to convergence.

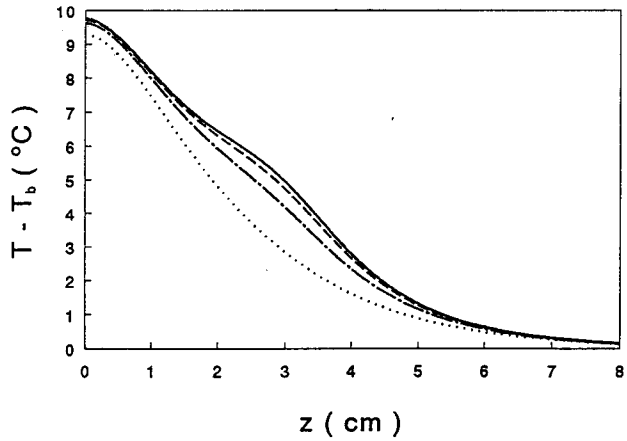

Figure 12. Temperature distribution for microwave (915 MHz) heating with the blood perfusion parameter as shown in Figure 11. Dot line: result of the zeroth order perturbation $T^{st(0)}(z)$, which is the same as what is shown in Figure 8. Dash-dotted line: result of the first order perturbation $T^{st(1)}(z)$. Dash line: result of the second order perturbation $T^{st(2)}(z)$. Solid line: result of the third order perturbation $T^{st(3)}(z)$.

10. Conclusions

A comprehensive framework for solving the bioheat equation is established using the time-dependent Green's function and Fourier transform techniques. It can be further extended to include the effects of spacially dependent tissue density, heat capacity, and thermal conductivity, in a way similar to that described in § 9. However, for treatment planning and machine design evaluation of localized heating methodologies, the theory in its present form is sufficient.

The primary advantage of the Green's function approach is that it provides opportunities for deriving analytic results. It also provides a unified view of both the steady state and the transient data. Such an approach can thus be a very useful alternative (or complement) to other methods such as the finite difference and the finite element techniques, especially for localized heating schemes where the variations of tissue parameters are small over the region of interest. It is less useful if the region of interest is large and contains large variations or discontinuities of the tissue parameters.

None of the examples presented are computationally intensive. The modelling of the interstitial RF system is the most time-consuming and requires the use of FFT. But even in this case it takes only 2 min on an IBM PC 386DX to generate a temperature distribution on a 64 by 64 grid. The modelling of the thermal conduction hyperthermia system takes even less time since the solution for an N needle configuration requires only the solution of a system of N linear equations. Such implementations therefore have the potential for online use during a hyperthermia treatment to model treatment parameters. While the clinical utility of such an approach has yet to be established, the computational methodology described here is not prohibitive.

Appendix

This appendix provides more details on the derivation of (9) which is the Fourier transform of (8).

Both spacial integrals on the right hand side of (8) are convolution integrals, i.e. they are both of the form

$$\int d^3x' g(\mathbf{x}')h(\mathbf{x}-\mathbf{x}'), \tag{68}$$

where $g(\mathbf{x})$ is equal to $T_0(\mathbf{x})$ for the first integral and $Q(\mathbf{x}, t)$ for the second integral, and

$$h(\mathbf{x}) = \exp(-\mathbf{x}^2/\beta),$$

with β being $4\alpha t$ for the first integral and $4\alpha(t-t')$ for the second integral.

Recall that the Fourier transform of a convolution integral (68) is

$$\tilde{g}(\mathbf{s})\tilde{h}(\mathbf{s}), \tag{69}$$

which follows directly from the definitions of the Fourier transform as given by (10) and (11). To arrive at (9), we need further the Fourier transform of $h(\mathbf{x})$:

$$\tilde{h}(\mathbf{s}) = \int d^3x e^{i\mathbf{s}\cdot\mathbf{x}} \exp(-\mathbf{x}^2/\beta), \tag{70}$$

which is most conveniently calculated in spherical coordinates as follows. Defining $r \equiv |\mathbf{x}|$ and $s \equiv |\mathbf{s}|$, we have

$$\begin{aligned}\tilde{h}(\mathbf{s}) &= \int_0^\infty dr 2\pi r e^{-r^2/\beta} \int_0^\pi d\theta \sin\theta e^{isr\cos\theta} \\ &= \int_0^\infty dr 2\pi r^2 e^{-r^2/\beta} \int_{-1}^1 d\xi e^{isr\xi} \\ &= \int_0^\infty dr 2\pi r e^{-r^2/\beta} (is)^{-1}(e^{isr} - e^{-isr}).\end{aligned} \tag{71}$$

Since the integrand in (71) is a even function of r, we can rewrite it as

$$\begin{aligned}\tilde{h}(\mathbf{s}) &= (\pi/s)i^{-1} \int_{-\infty}^\infty d\xi \xi e^{-\xi^2/\beta}(e^{is\xi} - e^{-is\xi}) \\ &= (2\pi/s) Im\left[\int_{-\infty}^\infty d\xi \xi e^{-\xi^2/\beta + is\xi}\right],\end{aligned} \tag{72}$$

where *Im* means taking the imaginary part. The integral in (72) can already be found in tables (see e.g. Gradshteyn and Ryzhik 1980). Or one can derive it as follows.

$$\begin{aligned}\int_{-\infty}^\infty d\xi \xi e^{-\xi^2/\beta + is\xi} &= e^{-\beta s^2/4} \int_{-\infty}^\infty d\xi (\xi - i\beta s/2) e^{-(\xi - i\beta s/2)^2/\beta} + i(\beta s/2) e^{-\beta s^2/4} \\ &\quad \int_{-\infty}^\infty d\xi e^{-(\xi - i\beta s/2)^2/\beta} \\ &= e^{-\beta s^2/4} \int_{-\infty}^\infty d\xi \xi e^{-\xi^2/\beta} + i(\beta s/2) e^{-\beta s^2/4} \int_{-\infty}^\infty d\xi e^{-\xi^2/\beta}.\end{aligned} \tag{73}$$

The first integral in (73) gives zero since its integrand is odd in ξ. For the second term we can use the familiar result:

$$\int_{-\infty}^\infty d\xi e^{-\xi^2/\beta} = (\pi\beta)^{1/2}, \tag{74}$$

which may be the integral that is most often encountered in the solution of heat transfer equations. The trick for doing this integral can be found in Feynman (1972). We thus arrive at

$$\int_{-\infty}^{\infty} d\xi \xi e^{-\xi^2/\beta + is\xi} = i(\pi^{1/2}\beta^{3/2}s/2)e^{-\beta s^2/4}. \tag{75}$$

Substituting this integral into (72) we obtain

$$\tilde{h}(\mathbf{s}) = (\pi\beta)^{3/2}e^{-\beta s^2/4}. \tag{76}$$

With the help of (68), (69) and (76), (9) follows directly from the Fourier transform of (8). Lastly, we note that (9) can also be derived by taking the Fourier transform of (2).

References

ABRAMOWITZ, M. and STEGUN, M. A. (eds), 1964, *Handbook of Mathematical Functions With Formulas, Graphs, and Mathematical Tables* (National Bureau of Standards).

CORRY, P. M., GERSTEN, D., LANGER, S. and MARTINEZ, A., 1993, Thermobrachytherapy: requirements for the future. *Medical Radiology, Interstitial and Intracavitary Thermoradiotherapy*, edited by M. H. Seegenschmiedt and R. Sauer (Berlin: Springer-Verlag), pp. 373–379.

DEFORD, J. A., BABBS, C. F., PATEL, U. H., FEARNOT, N. E., MARCHOSKY, J. A. and MORAN, C. J., 1990, Accuracy and precision of computer-simulated tissue temperatures in individual human intracranial tumours treated with interstitial hyperthermia. *International Journal of Hyperthermia*, **6**, 771–784.

FEYNMAN, R. P., 1972, *Statistical Mechanics* (London: Benjamin/Cummings), 29 pp.

GRADSHTEYN, I. S. and RYZHIK, I. M., 1980, *Table of Integrals, Series, and Products* (New York: Academic Press), 338 pp.

JACKSON, J. D., 1975, *Classical Electrodynamics* (New York: Wiley).

MARTINEZ, A., GERSTEN, D. and CORRY, P. M., 1993, Clinical rationale for interstitial thermoradiotherapy of cynecological tumors: review of clinical results and own experiences with continuous mild hyperthermia. *Medical Radiology, Interstitial and Intracavitary Thermoradiotherapy*, edited by M. H. Seegenschmiedt and R. Sauer (Berlin: Springer-Verlag), pp. 179–185.

NEWMAN, W. H., LELE, P. P. and BOWMAN, H. F., 1990, Limitations and significance of thermal washout data obtained during microwave and ultrasound hyperthermia. *International Journal of Hyperthermia*, **6**, 771–784.

PENNES, H. H., 1948, Analysis of tissue and arterial blood temperatures in the resting forearm. *Journal of Applied Physiology*, **1**, 93–122.

PRESS, W. H., TEUKOLSKY, S. A., VETTERLING, W. T. and FLANNERY, B. P., 1992, *Numerical Recipes in C: The Art of Scientific Computing* (Cambridge: Cambridge University Press).

WATERMAN, F. M., TUPCHONG, L. and LIU, C. R., 1991, Modified thermal clearance technique for determination of blood flow during local hyperthermia. *International Journal of Hyperthermia*, **7**, 719–733.